

Abstract

The complexity of biological systems demands the use of appropriate controllers in order to control the final quality of the system based on the effects of inputs of the system. Wound healing is a complex biological process dependent on multiple variables: tissue oxygenation, wound size, on muen]

***Corresponding authors:** Aydin Azizi, Department of Engineering, German University of Technology, Muscat, Oman, Tel: 968 22 061111; E-mail: aydin.azizi@gutech.edu.com

Received July 19, 2017; **Accepted** September 08, 2017; **Published** September 12, 2017

Citation: Azizi A (2017) Designing of Artificial Intelligence Model-Free Controller Based on Output Error to Control Wound Healing Process. Biosens J 6: 147. doi:[10.4172/2090-4967.1000147](https://doi.org/10.4172/2090-4967.1000147)

Copyright: © 2017 Azizi A. This is an open-access article distributed under the terms of the Creative Commons Attribution License, which permits unrestricted use, distribution, and reproduction in any medium, provided the original author and source are credited.

Wound repair progresses through several overlapping phases which include inflammation, proliferation and remodeling (Figure 1) [9,10]. The final outcome and the entire process are pretty sensitive to the

interact in a very complicated manner with nonlinear feedback. Such complex feedback mechanisms can be easily addressed by mathematical modeling. There are certain assumptions taken into account when formulating the following models. These assumptions are a few well-known interactions which are briefly summarized.

Firstly, the orientation of the matrix tends to direct fibroblast movement. This is a phenomenon called "Contact Guidance" [19-21]. Secondly, the speed of the fibroblasts is affected by the ECM. It is proven that the matrix composition has an effect on the mobility of fibroblasts that migrate more easily on fibronectin gels than on collagen gels [22]. Thirdly, the production of different proteins by the fibroblasts is highly sensitive to the composition of the ECM [23,24]. Fourth, a plethora of growth factors and cytokines that alter fibroblast behavior can be found in the ECM in the wound region. Finally, fibroblasts tend to organize the thin collagen fibrils into the fibrous structure noticeable in the dermis [19].

Two of these interactions are of great importance to our models and require more explanation. Firstly, the "Contact Guidance" has been proven directly when fibroblasts put on oriented collagen gels attack the gels in the direction of orientation [25]. More proof to this behavior can be observed when fibroblasts migrate along fibronectin fibrils [26]. The next key interaction is associated to the way collagen is produced by fibroblasts and the complex process by which the collagen polymerizes to form a fibrous network of matrix [27]. Fibroblasts release procollagen molecules through secretory vesicles. Deep, narrow recesses in the fibroblasts' cell surface are created by the fusion of these vesicles with the cell membrane. These collagen fibrils are formed in these recesses. There is a theory that these deep recesses provide the fibroblasts with the control over the micro-environment in which the collagen fibrils are forming and therefore control over the structure of the resulting collagen matrix [28].

The collagen matrix is itself considered to be an important framework used by migrating fibroblasts as scaffolding to crawl on. Therefore, as the fibroblasts affect the orientation of the matrix, the matrix orientation influences the directed movement of the fibroblasts.

Extracellular matrix remodeling in soft connective tissues is induced by both biochemical and biomechanical stimuli [13,29]. The morphology and (mechanical) behavior of the stimulated tissue is greatly affected by the remodeling process [30]. Mechanically induced extracellular matrix remodeling is an important role player in tissue engineering of load-bearing structures, such as cartilage [31] and heart valves [32].

A mathematical model is necessary to have a deeper understanding of the processes of tissue remodeling. The model should include both the causes and consequences of the remodeling processes. It can easily be observed that this model acts as a useful tool for tissue engineering applications to optimize the mechanical conditioning protocol and to acquire the desired tissue integrity; efficient protocols cannot be designed unless an understanding of the tissue's response to mechanical stimuli is gained. These protocols may be of great assistance in manipulating the process of remodeling toward the desired result.

The model of dermal wound healing that we use here is a model of fibroblasts cells [33]. In this research attempted to represent the cells (n) as independent entities owing to the scales involved.

A typical mobile fibroblast can have different lengths ranging values of the order 100 nm, and the diameters of the collagen fibers are of the order 1 μm [28,34]. In addition, what makes the independent

representation more realistic is that normal dermal tissue is relatively sparsely populated with cells. It should also be noted that during wound healing more cells are employed to the region.

The cell conservation equation is:

$$\frac{\partial n}{\partial t} + \nabla_x \left(\frac{\partial u}{\partial t} \right) - 2D \frac{\partial^2 n}{\partial x^2} = 2r m(n_0 - 4n) \quad (3.1)$$

Boundary conditions (B.C) of (1) are:

$$n(0, t) = 0 \quad n(x, 0) = 0$$

To solve (3.1) as told before we consider the wound shape as a circle with $R=l/2$, at first, we suppose R as an interval named an element (e) (Figure 3) and then we will extend R to more elements.

Now we write weak form integration for this element as seen below:

$$\int_1^2 | 0$$

$$N_1 \mid \frac{x_2 \ 4 \ x}{L} \Downarrow \dot{N}_1 \mid 4 \frac{1}{L} \quad (3.21)$$

$$N_2 \mid \frac{x \ 4 \ x_1}{L} \Downarrow \dot{N}_2 \mid \frac{1}{L} \quad (3.22)$$

With replacing (3.21) and (3.22) in (3.20):

$$\frac{2}{11} \cdot \dot{N}_i(\cdot) \dot{N}_i(\cdot) \mid 4 \frac{1}{L} \quad 2 \frac{1}{L} \quad 2$$

$$\int_{x_1}^{x_2} N_2^3 dx \Big| \frac{(x_2 - x_1)^4}{4L^3} \Big|_{x_1}^{x_2} \Big| \frac{L}{4} \tag{3.45}$$

$$\int_{x_1}^{x_2} N_1^2 dx \Big| \left(\frac{41}{3L^2} (x_2 - x_1)^3 \right) \Big|_{x_1}^{x_2} \Big| \frac{L}{3} \tag{3.46}$$

$$\int_{x_1}^{x_2} N_2^2 dx \Big| \left(\frac{(x_2 - x_1)^3}{3L^2} \right) \Big|_{x_1}^{x_2} \Big| \frac{L}{3} \tag{3.47}$$

$$\begin{aligned} & \int_{x_1}^{x_2} N_1 N_2 dx \Big| \int_{x_1}^{x_2} \frac{x(x_2 - x_1) - 4x^2 - 4x_1 x_2}{L^2} dx \\ & \Big| \frac{1}{L^2} \left(\frac{x^2}{2} (x_2 - x_1) - 4 \frac{x^3}{3} - 4x_1 x_2 x \right) \Big|_{x_1}^{x_2} \\ & \Big| \frac{1}{L^2} \left(\frac{x_2^2}{2} (x_2 - x_1) - 4 \frac{x_2^3}{3} - 4x_1 x_2^2 - 4 \frac{x_1^2}{2} (x_2 - x_1) - 2 \frac{x_1^3}{3} - 2x_1^2 x_2 \right) \Big|_{x_1}^{x_2} \\ & \Big| \frac{1}{L^2} \left(\frac{L^2}{2} \Delta L - 4 \frac{L^3}{3} + 40402020 \right) \\ & \Big| \frac{1}{L^2} \left(L^3 \left(\frac{1}{2} - 4 \frac{1}{3} \right) \right) \Big| \frac{L}{6} \tag{3.48} \end{aligned}$$

$$\begin{aligned} & \int_{x_1}^{x_2} N_1^2 N_2 dx \Big| \int_{x_1}^{x_2} \frac{(x_2 - x_1)^2 (x_2 - x_1)}{L^3} dx \\ & \Big| \frac{1}{L^3} \int_{x_1}^{x_2} (x_2^2 - 4x_2 x_1 + 2x_1^2) (x_2 - x_1) dx \\ & \Big| \frac{1}{L^3} \int_{x_1}^{x_2} (x_2^2 x - 4x_1 x_2^2 + 4x_2 x_1^2 - 2x_2 x_1 + 2x_1^3 - 4x_1 x_2^2) dx \\ & \Big| \frac{1}{L^3} \left(x_2^2 \frac{x^2}{2} - 4x_1 x_2^2 x + 4x_2 \frac{x^3}{3} - 4x_2 x_1^2 \frac{x^2}{2} - 2 \frac{x^4}{4} - 4x_1 x_2^2 x \right) \Big|_{x_1}^{x_2} \\ & \Big| \frac{1}{L^3} \left(\frac{L^4}{2} - 404 \frac{2}{3} L^4 + 402 \frac{L^4}{4} - 40 \right) \\ & \Big| \frac{1}{L^3} \left(\frac{1}{2} - 4 \frac{2}{3} + 2 \frac{1}{4} \right) L^4 \Big| \frac{L}{12} \tag{3.49} \end{aligned}$$

$$\begin{aligned} & \int_{x_1}^{x_2} N_1 N_2^2 dx \Big| \int_{x_1}^{x_2} \frac{(x_2 - x_1) \Delta (x_2 - x_1)^2}{L^3} dx \\ & \Big| \frac{1}{L^3} \int_{x_1}^{x_2} (x_2 - x_1) (x_2^2 - 4x_2 x_1 + 2x_1^2) dx \\ & \Big| \frac{1}{L^3} \int_{x_1}^{x_2} (x_2 x^2 - 4x_2 x_1 x + 2x_2 x_1^2 - 4x^3 + 4x_2 x_1^2 - 4x_1^2 x) dx \\ & \Big| \frac{1}{3} \left(\frac{2}{3} - 4 \frac{2}{2} + 2 \frac{2}{2} - 2 \frac{2}{1} + 4 \frac{4}{4} - 4 \frac{2}{1} + 2 \frac{2}{1} - 4 \frac{2}{1} \frac{2}{2} \right) \Big|_{x_1}^{x_2} \Big| \frac{L}{10} \end{aligned}$$

With replacing (3.66) in (3.65):

$$\begin{pmatrix} \dot{n}_1 \\ \dot{n}_2 \end{pmatrix} = \begin{bmatrix} -4A^{41} & DB \\ 4A^{41}rC & -4A^{41}rV - 2A^{41}DB \end{bmatrix} \begin{pmatrix} n_1 \\ n_2 \end{pmatrix} \quad (3.67)$$

$$\vec{n}_j(i+1) = \vec{n}_j(i) + h\vec{f}(t(i), n_1, n_2) \quad (3.68)$$

j

1 2
1 2 1

solid vertical bar at the left. The dimensions of P are displayed below the variable as 4×1 , indicating that the input is a single vector of 4 elements:

$$\begin{pmatrix} \cdot \\ \cdot \\ \cdot \\ \cdot \end{pmatrix}, \quad \begin{matrix} 1,2,3, \\ 100 \end{matrix}$$

$$e = \frac{1}{2}(y_j^d - 4y_j)^2 \quad (4.11)$$

$$\frac{\partial e}{\partial w_{ji}} = 4\xi \frac{\partial e}{\partial w_{ji}} \quad (4.12)$$

$$w^{new} = w^{old} + 2 \frac{\partial e}{\partial w} \quad (4.13)$$

$$\frac{\partial e}{\partial b} = 4\xi \frac{\partial e}{\partial b} \quad (4.14)$$

$$b^{new} = b^{old} + 2 \frac{\partial e}{\partial b} \quad (4.15)$$

So, in each layer to find w^{new} and b^{new} , at first, we should calculate

$\frac{\partial e}{\partial b}$ and $\frac{\partial e}{\partial w}$.

Hidden layer:

a) Computing w^{new} :

From (4.11) we know:

$$\frac{\partial e}{\partial w^1} = 4\xi \frac{\partial e}{\partial w^1} \Downarrow \frac{\partial e}{\partial w^1} = \frac{\partial e}{\partial y} \Delta \frac{\partial y}{\partial n^2} \Delta \frac{\partial n^2}{\partial a^1} \Delta \frac{\partial a^1}{\partial n^1} \Delta \frac{\partial n^1}{\partial w^1} \quad (4.16)$$

$$e = \frac{1}{2}(y^{desired} - 4y)^2 \Downarrow \frac{\partial e}{\partial y} = 4(y^{desired} - 4y) \quad (4.17)$$

$$y = f(n^2) = \text{purelin}(n^2) = n^2 \Downarrow \frac{\partial y}{\partial n^2} = f'(n^2) = 1 \quad (4.18)$$

$$n^2 = -w^2 a^1 + 2b^1 \Downarrow \frac{\partial n^2}{\partial a^1} = w^2 \quad (4.19)$$

$$\frac{\partial a^1}{\partial n^1} = f'(n^1) = 14 \frac{\exp(n^1) - 4 \exp(4n^1)}{(\exp(n^1) + 2 \exp(4n^1))^2} \quad (4.20)$$

$$\frac{\partial n^1}{\partial w^1} = p \quad (4.21)$$

With substituting (4.17)-(4.21) in (4.16):

$$\frac{\partial e}{\partial w^1} = 4(y^{desired} - 4y) \Delta w^2 \Delta (14 \frac{\exp(n^1) - 4 \exp(4n^1)}{(\exp(n^1) + 2 \exp(4n^1))^2} \Delta p \quad (4.22)$$

$$\frac{\partial e}{\partial w^1} = \xi (y^{desired} - 4y) \Delta w^2 \Delta (14 \frac{\exp(n^1) - 4 \exp(4n^1)}{(\exp(n^1) + 2 \exp(4n^1))^2} \Delta p \quad (4.23)$$

So we can now compute w^{new} with replacing (4.23) in (4.13):

$$w^{1new} = w^{1old} + 2 \frac{\partial e}{\partial w^1} \quad (4.24)$$

b) Computing b^{new} :

$$\frac{\partial e}{\partial b^1} = 4\xi \frac{\partial e}{\partial b^1} \Downarrow \frac{\partial e}{\partial b^1} = \frac{\partial e}{\partial y} \Delta \frac{\partial y}{\partial n^2} \Delta \frac{\partial n^2}{\partial a^1} \Delta \frac{\partial a^1}{\partial n^1} \Delta \frac{\partial n^1}{\partial b^1} \quad (4.25)$$

$$n^1 = -w^1 p + 2b^1 \Downarrow \frac{\partial n^1}{\partial b^1} = 1 \quad (4.26)$$

With replacing (4.17)-(4.20) and (4.26) in (4.25):

$$\frac{\partial e}{\partial b^1} = 4(y^{desired} - 4y) \Delta w^2 \Delta (14 \frac{\exp(n^1) - 4 \exp(4n^1)}{(\exp(n^1) + 2 \exp(4n^1))^2} \Delta p \Delta 1$$

Control of Wound Healing Process Using Neural Networks

Almost all tissue types have the ability to adapt to changes in the applied load, according to Wolff's law [36]. Cells maintain the matrix and they are the key modulators of mechanically-induced tissue formation and remodeling, and in this way actively control tissue architecture and mechanics to adapt to changes in functional demands. Cells can reorganize and remodel the extracellular matrix by changing the production of matrix components, by secreting matrix enhancing or degrading products and their inhibitors, and by applying (traction) forces to the deposited fibers. At the moment, it is not exactly known how the cells sense and affect their environment, but several cellular mechano sensors and mechano transduction pathways have been proposed [37,38].

It is generally accepted that collagen synthesis, accumulation and organization are increased by mechanical stimuli, resulting in improved mechanical properties of the tissue. Cyclic strain increased the production of collagen in engineered smooth muscle tissue [39] and the rate of collagen synthesis was increased in mechanically stimulated pulmonary arteries [40]. Collagen content also increased in long-term tissue-engineered vascular structures [41] and in axially stretched carotid arteries [42]. Pulmonary fibroblasts also showed an increased collagen expression when stimulated mechanically.

Increasing collagen content means increasing number of fibroblasts [33], so it can be said cell density (fibroblast density) can be increased by mechanical stimuli. This stimulation can be electrical stimulation or effect of magnetic fields on wounded area.

With these descriptions we use effect of mechanical stimuli at the wounded area to control the healing process. We suppose this stimulation is the force which is result of exposing skin in electrical or magnetic fields and effect of this force is cell production. We suppose the relationship between the exerted force to skin and cell production is a linear function as seen below:

$$n_f = \frac{1}{2} F + N(0,1) \Delta 10^{44} + \Delta(n_0 + 4n) \quad (5.1)$$

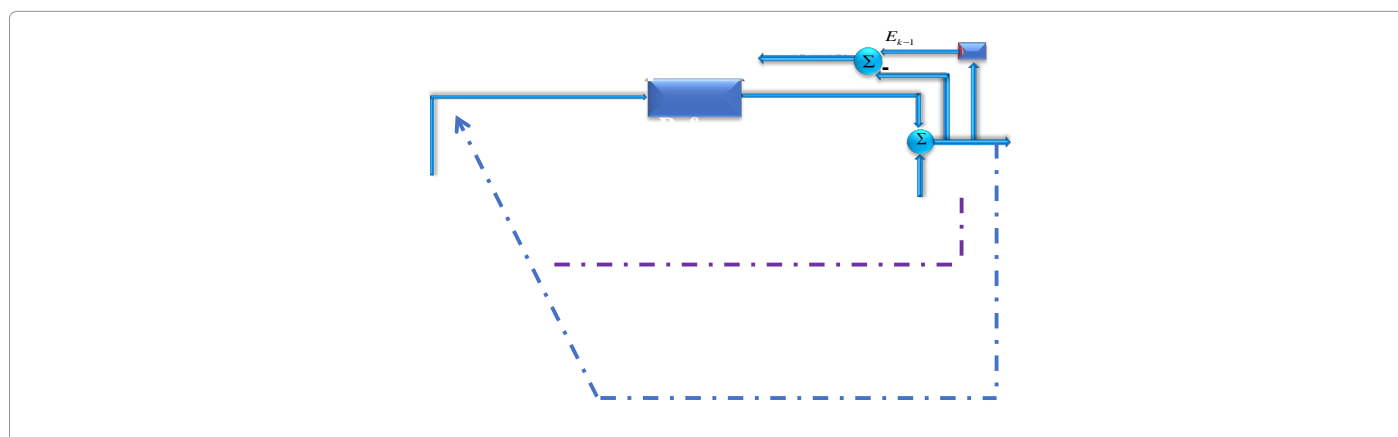
Which $N(0,1)$ is normal distribution with average zero and variance one.

n_f is produced cell by exerted force to wound area, n_0 is unwounded skin cell amount and n is cell amount which is produced by normal healing process and obtained from (3.1).

To control wound healing process (Figure 16) two networks are used, first one to simulate the plant and the second one acts as controller. These neural networks are two-layer networks; each layer has its own weight matrix W , its own bias vector b , the neural network used as plant's approximators has one input and one output and the other neural network used as controller has two inputs and one output. We will use superscripts to identify the layers. Specifically, we append the number of the layer as a superscript to the names for each of these variables. Thus, the weight matrix for the first layer is written as W^1 , and the weight matrix for the second layer is written as W^2 .

Wound healings simulator

To model the plant, as told previously, consider a one hidden layer-network (Figures 16 and 17). This network has one input buffer (F) and



single output (n). This network is trained online by getting force (F) data information executed from neural network controller, and approximates amount of cell (n) as networks output. Error will calculate by comparing neural network's output with plant's output as desired output. Desired output can be obtained in two ways:

1. Using data information which is obtained by experience in real world.
2. Using appropriate mathematical model.

For our purpose we choose the second one, so use mathematical model which introduced before, but this technique is established for real data instead of mathematical model. Nodes' weights and biases are updated by using error back propagation method and chain rule is written as same fashion as told before in section 4.

So input, output, bias and weight matrixes are defined (Figure 17).

$$P \mid F(x,t) \tag{5.2}$$

$$W^1 \mid \begin{pmatrix} w_{1,1} \\ w_{1,2} \\ w_{1,3} \\ w_{1,4} \\ w_{1,5} \end{pmatrix} \tag{5.3}$$

$$b^1 \mid \begin{pmatrix} b_1 \\ b_2 \\ b_3 \\ b_4 \\ b_5 \end{pmatrix} \tag{5.4}$$

$$W^2 \mid \{w_{1,1} \ w_{2,1} \ w_{3,1} \ w_{4,1} \ w_{5,1}\} \tag{5.5}$$

$$b^2 \mid \{b_1 \ b_2 \ b_3 \ b_4 \ b_5\} \tag{5.6}$$

$$y \mid n(x,t) \tag{5.7}$$

Chain rules to back-propagate the error is written in the same fashion seen in section 4.

Controller design

We choose model reference control (MRC) architecture to design neural network controller. This MRC controller is designed in the same fashion as plant approximator's network. The controller's network has two inputs, first one is error in kth time step (E_k) which is calculated from difference between output of controlled plant, Cell (n), and amount of cell exists in unwounded (normal) skin (model reference), and the other one is derivative of E_k with respect to time (dE_k) (Figure 18).

As told before the output of controller is force (F)

1

With replacing (5.19)-(5.24) and (5.36)-(5.38) in (5.35):

$$\frac{\epsilon E}{\epsilon W_{controller}^1} \mid 4 y_{model} \Delta w_{model}^2 \Delta (14 (exp(n_{model}^1) 4 exp(4n_{model}^1))^2 / (exp(n_{model}^1) 2 exp(4n_{model}^1))^2) \Delta w_{model}^1 \Delta w_{controller}^2 \Delta (14 (exp(n_{controller}^1) 4 exp(4n_{controller}^1))^2 / (exp(n_{controller}^1) 2 exp(4n_{controller}^1))^2) \Delta P_{controller} \tag{5.39}$$

With replacing (5.39) in (4.12):

$$\div w_{controller}^1 \mid \xi \Delta y_{model} \Delta w_{model}^2 \Delta (14 (exp(n_{model}^1) 4 exp(4n_{model}^1))^2 / (exp(n_{model}^1) 2 exp(4n_{model}^1))^2) \Delta w_{model}^1 \Delta w_{controller}^2 \Delta (14 (exp(n_{controller}^1) 4 exp(4n_{controller}^1))^2 / (exp(n_{controller}^1) 2 exp(4n_{controller}^1))^2) \Delta P_{controller} \tag{5.40}$$

with replacing (5.40) in (4.13):

$$w_{controller}^{1new} \mid w_{controller}^{1old} 2 \div w_{controller}^1 \tag{5.41}$$

Computing $b_{controller}^{2new}$:

20) error of plant's neural network in each time step (day) converge to zero it means that in each day plant's neural network show the behavior as plant (mathematical model). In this moment which controller is trained we can eliminate the model's neural network and test controller's network.

Conclusion

Control of wound healing by neural networks is a new idea discussed here as Bio-Control science. In this research we design a model free

